Journal of Power Sources 183 (2008) 741–748

Contents lists available at ScienceDirect

Journal of Power Sources

journal homepage: www.elsevier.com/locate/jpowsour

Effect of $FePO_4$ coating on electrochemical and safety performance of $LiCoO_2$ as cathode material for Li-ion batteries

Gang Li, Zhanxu Yang, Wensheng Yang*

State Key Laboratory of Chemical Resource Engineering, Beijing University of Chemical Technology, Beijing 100029, PR China

ARTICLE INFO

Article history:
Received 27 January 2008
Received in revised form 18 May 2008
Accepted 19 May 2008
Available online 23 May 2008

Keywords:
Lithium-ion battery
Cathode material
$LiCoO_2$
$FePO_4$ coating
Safety

ABSTRACT

$LiCoO_2$ was surface modified by a coprecipitation method followed by a high-temperature treatment in air. $FePO_4$-coated $LiCoO_2$ was characterized with various techniques such as X-ray diffraction (XRD), auger electron spectroscopy (AES), field emission scanning electron microscope (FE-SEM), energy dispersive spectroscopy (EDS), transmission electron microscope (TEM), electrochemical impedance spectroscopy (EIS), 3 C overcharge and hot-box safety experiments. For the 14500R-type cell, under a high charge cutoff voltage of 4.3 and 4.4 V, 3 wt.% $FePO_4$-coated $LiCoO_2$ exhibits good electrochemical properties with initial discharge specific capacities of 146 and 155 mAh g^{-1} and capacity retention ratios of 88.7 and 82.5% after 400 cycles, respectively. Moreover, the anti-overcharge and thermal safety performance of $LiCoO_2$ is greatly enhanced. These improvements are attributed to the $FePO_4$ coating layer that hinders interaction between $LiCoO_2$ and electrolyte and stabilizes the structure of $LiCoO_2$. The $FePO_4$-coated $LiCoO_2$ could be a high performance cathode material for lithium-ion battery.

1. Introduction

Among various cathode materials, layered $LiCoO_2$ is the most widely used in commercial Li-ion batteries due to its high energy density, high operating voltage and good electrochemical performance with charge cutoff voltage lower than 4.2 V [1–3]. The capacity of Li-ion batteries, 18650R-type as an example, has been increased from 1200 mAh in 1991 to 2600 mAh (500 mAh cm^{-3}) in 2005. However, such a high capacity enhancement should be mainly achieved by maximum utilizing the cell dead space, modifying the thickness of the current collector and decreasing the amounts of binder and conducting agent in the electrodes [4]. In order to obtain higher specific capacity of $LiCoO_2$ material, the charge cutoff voltage has to be increased beyond 4.2 V. However, when the charge cutoff voltage increases to 4.4 from 4.2 V, the x in Li_xCoO_2 decreased from 0.45 to 0.3, resulting in a rapid capacity loss and a large anisotropic volume change of over 3% because of the phase transition among hexagonal, monoclinic, and H1-3 phases. Furthermore, highly oxidized Co^{4+} ions are apt to decompose electrolyte in the particle surface, resulting in substantial amounts of gas generation [5].

In order to overcome the problems mentioned above, partial substitution of Co with other metals, such as Al, Mg, and Zn, has been extensively studied [6–8]. However, capacity fading has been still observed even though some improvements have been achieved [8]. As an alternative, there has been an extensively research by coating cathode material with metal oxides such as MgO [9], Al_2O_3 [10], CeO_2 [11], ZrO_2 [12] and TiO_2 [3]. These inert oxide coating materials on the surface of the cathode particles can limit the direct contact of the active material with the electrolyte, and thus prevent dissolution of cobalt in the electrolyte [13]. Some authors also suggested that the coating materials form solid solution phase $LiCo_{1-x}M_xO_2$ (M = Al, Zn, Sn [14–16]), which improves structural stability of the core material and enhances its cycling performance. However, Wang et al. [17] reported that despite the superior electrochemical properties, the thermal stability of the metal oxide-coated $LiCoO_2$ is poor when cycled at high temperature and during the overcharge test. So, they used $LiFePO_4$ as the coating material, the thermal stability and electrochemical performance of $LiFePO_4$-coated $LiCoO_2$ is improved. But it is well-known that the synthesis of $LiFePO_4$ needs nitrogen as protective atmosphere, while the structure of $LiCoO_2$ would be more or less damaged during high-temperature process in the atmosphere short of oxygen.

Recently, it was reported that $FePO_4$ is a promising 3 V cathode material for Li-ion batteries because of its various advantages such as environmental friendliness, low cost and thermal stability [18–20]. Considering the advantages of $FePO_4$, we report here our investigations about the effect of $FePO_4$ coating on electrochemical and safety performance of $LiCoO_2$. The $LiCoO_2$ was surface modified

* Corresponding author. Tel.: +86 10 6443 5271; fax: +86 10 6442 5385.
E-mail address: yangws@mail.buct.edu.cn (W. Yang).

0378-7753/$ – see front matter © 2008 Elsevier B.V. All rights reserved.
doi:10.1016/j.jpowsour.2008.05.047

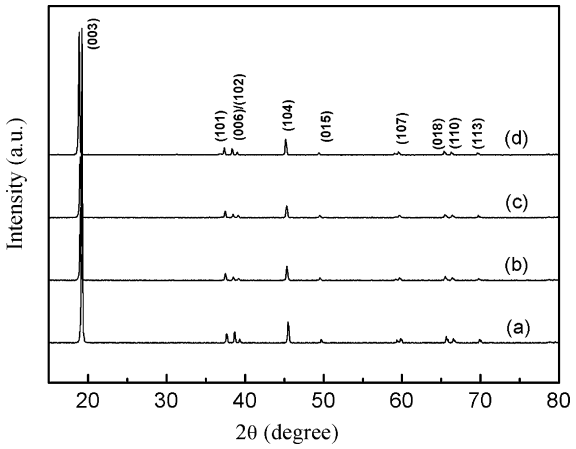

Fig. 1. X-ray diffraction patterns of different amounts of $FePO_4$-coated $LiCoO_2$: (a) 0 wt.%, (b) 1 wt.%, (c) 3 wt.% and (d) 5 wt.%.

by a coprecipitation method followed by a high-temperature treatment in air. We employed various analytical techniques such as X-ray diffraction (XRD), auger electron spectroscopy (AES), field emission scanning electron microscope (FE-SEM), energy dispersive spectroscopy (EDS), transmission electron microscope (TEM) and electrochemical impedance spectroscopy (EIS) to understand the mechanism of the improvement in the electrochemical properties of the $FePO_4$-coated $LiCoO_2$ material. In addition, 3 C overcharge and hot-box safety experiments were used to study the effect of $FePO_4$ coating layer on the safety performance of $LiCoO_2$.

2. Experimental

2.1. Synthesis of $FePO_4$-coated $LiCoO_2$ cathode materials

Commercial $LiCoO_2$ (Beijing Easpring Company) with average particle size of 10 μm was used as the pristine material. Reagent grade $Fe(NO_3)_3{\cdot}9H_2O$ and $(NH_4)_2HPO_4$ were selected as the starting materials for the coating layers. $LiCoO_2$ was dispersed into the $Fe(NO_3)_3$ solution and ultrasonically agitated for 30 min. Then, the suspension was stirred mechanically while $(NH_4)_2HPO_4$ solution was slowly dropped into it. The final powder was filtered and washed several times with distilled water, dried at 130 °C for 12 h, and subsequently heat-treated in a furnace at 550 °C for 10 h in air.

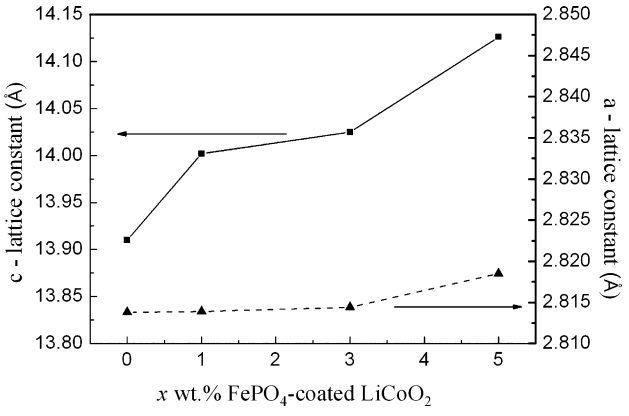

Fig. 2. Hexagonal lattice constants for 0, 1, 3 and 5 wt.% $FePO_4$-coated $LiCoO_2$.

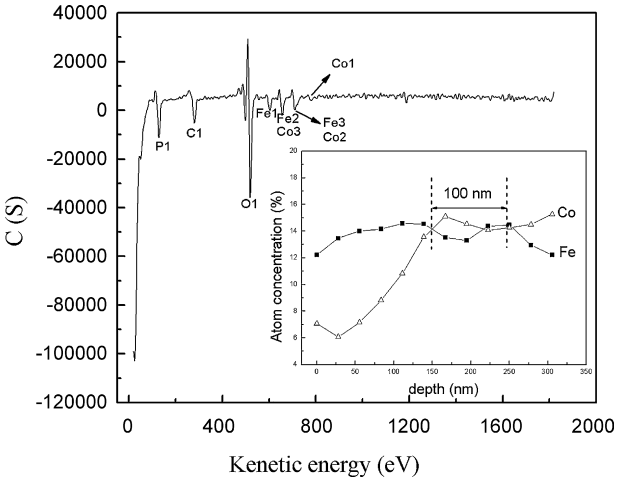

Fig. 3. Auger electron spectroscopy of 3 wt.% $FePO_4$-coated $LiCoO_2$ particles. The inset shows the depth profile of 3 wt.% $FePO_4$-coated $LiCoO_2$ particles.

2.2. Characterization of $FePO_4$-coated $LiCoO_2$ cathode materials

Powder X-ray diffraction (XRD, Shimadzu, XRD-6000) measurements using Cu Kα radiation were employed to identify the crystal structures of pristine $LiCoO_2$ and $FePO_4$-coated $LiCoO_2$ powder. XRD data were obtained at $2\theta = 15–80°$, with a step size of 0.02° and a count time of 4 s. From the XRD data, the lattice parameters were calculated by the least-squares method. Auger electron spectroscopy (AES, ULVAC-PHI, AES-PHI 700) was used to examine the spatial distributions of constituent ions in the coated particles. The morphologies of $FePO_4$-coated and uncoated $LiCoO_2$ materials were observed by field emission scanning electron microscope (FE-SEM, Hitachi, S-4700). The elemental distribution on the surface of the $FePO_4$-coated $LiCoO_2$ samples was studied by energy dispersive spectroscopy (EDS, EDAX, Genesis 60). The thickness of $FePO_4$ coating layer was examined using Transmission electron microscope (TEM, Hitachi, H-800).

2.3. Electrochemical measurements

For the electrochemical performance tests, the 14500R-type Li-ion batteries were used. The positive electrode was prepared by mixing the active material, acetylene black and PVDF binder in weight ratio of 90:4:6 in *N*-methyl-2-pyrrodidene (NMP) and then coating the cathode-slurry onto an Al foil, followed by drying at 130 °C for 20 min and roll-pressing. The negative electrode was prepared by mixing MCMB, acetylene black and PVDF binder in weight ratio of 90:2:8 in NMP and then coating the anode-slurry onto a Cu foil, followed by drying at 130 °C for 20 min and roll-pressing. The fabrication of cells was done in a dry room with an electrolyte of 1 mol L^{-1} $LiPF_6$ in EC-DMC-DEC (1:1:1 volume ratio) solution and a separator of Celgard 2400. The test cells were aged at room temperature for 24 h before electrochemical test was performed. Then the cells were charged and discharged between 2.75–4.3 and 4.4 V by applying a constant 1 C current at 25 °C.

For the electrochemical impedance spectroscopy (EIS) experiments, the 2032 coin-type cells with Li metal as the negative electrode were assembled in an argon-filled glove box. EIS experiments were performed in the charged state of 4.3 V (vs. Li/Li^+) for each cycle using a CHI 660C electrochemistry workstation (Shanghai Chenhua Instrument Co., China) over the frequency range from 1 MHz to 10 mHz with the amplitude of 5 mV.

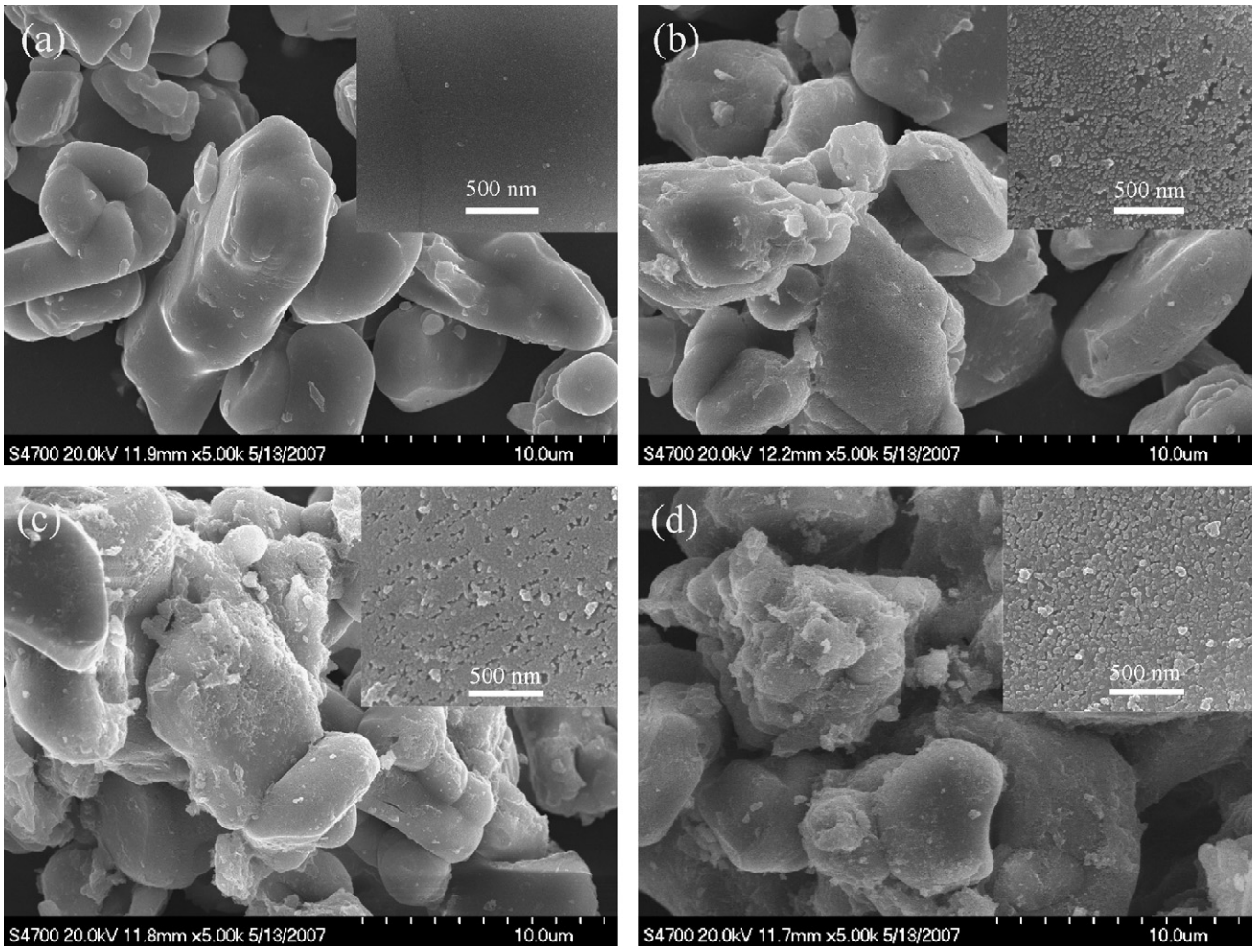

Fig. 4. FE-SEM images of different amounts of $FePO_4$-coated $LiCoO_2$: (a) 0 wt.%, (b) 1 wt.%, (c) 3 wt.% and (d) 5 wt.%.

2.4. Safety performance tests

For the safety performance tests, 3 C overcharge and hot-box experiments were performed. The 14500R-type test cells were cycled for three cycles between 2.75 and 4.2 V before testing. For the 3 C overcharge tests, the cells were charged to the critical voltage at a current of 3 C, and then maintained at that voltage until the current was decreased to 20 mA. For the hot-box experiments, the cells were charged to 4.2 V with a constant 1 C current and then held at 4.2 V until the current was decreased to 20 mA, then the charged cells were placed in a 145 °C oven.

3. Results and discussion

3.1. Crystal structure and surface morphology

The crystalline structures of the $FePO_4$-coated and uncoated $LiCoO_2$ particles were characterized by XRD (Fig. 1). The XRD patterns show that all the samples have a hexagonal α-$NaFeO_2$-layered structure ($R\,\bar{3}\,m$), which is based on a close-packed network of oxygen atoms with alternating Li and Co planes. The fact that no diffraction pattern corresponding to the coating material was observed is expected since the amount of coating material is very small and it exists as a thin film on the surface of $LiCoO_2$. In addition, compared with the pristine $LiCoO_2$, the (0 0 l) peaks of all the $FePO_4$-coated $LiCoO_2$ powders shift to the lower angle, while the change of other peaks is negligible. Lattice constants of uncoated and $FePO_4$-coated $LiCoO_2$ were calculated from the XRD patterns and the results are shown in Fig. 2. It is shown clearly that the c value of $FePO_4$-coated $LiCoO_2$ is much larger than that of the uncoated material, while the a value only slightly increases. The c-axis expansion indicates that some Co^{3+} ions are substituted by Fe^{3+} ions to form a $LiCo_{1-x}Fe_xO_2$ phase during calcination process [21]. In order to prove the above analysis, AES was used to investigate the spatial distributions of constituent ions in the coated particles, and the result is shown in Fig. 3. It is seen clearly that Co element on the top surface of 3 wt.% $FePO_4$-coated $LiCoO_2$ is hardly detected, which means that $LiCoO_2$ particles are completely encapsulated. The depth profile of Co in the inset of Fig. 3 shows that the concentration of Co increases sharply to a depth of ~160 nm and then levels off. The concentration of Fe changes very little to a depth of ~150 nm, levels off to a depth of 250 nm and then decreases. From the above results, we can determine that the thickness of $FePO_4$ coating layer is ~150 nm and that Fe is diffused into the bulk of $LiCoO_2$ during calcination process to form a Li–Co–Fe–O phase with a thickness of ~100 nm.

FE-SEM images of the uncoated and $FePO_4$-coated $LiCoO_2$ are shown in Fig. 4. Obviously the surface of the pristine $LiCoO_2$ is very smooth and seems rather "clean" without any radicals (Fig. 4a). After coated with 1 wt.% $FePO_4$, the morphology of the particles does not change obviously at low magnification (Fig. 4b). More detailed observation at high magnification shows that the surface of

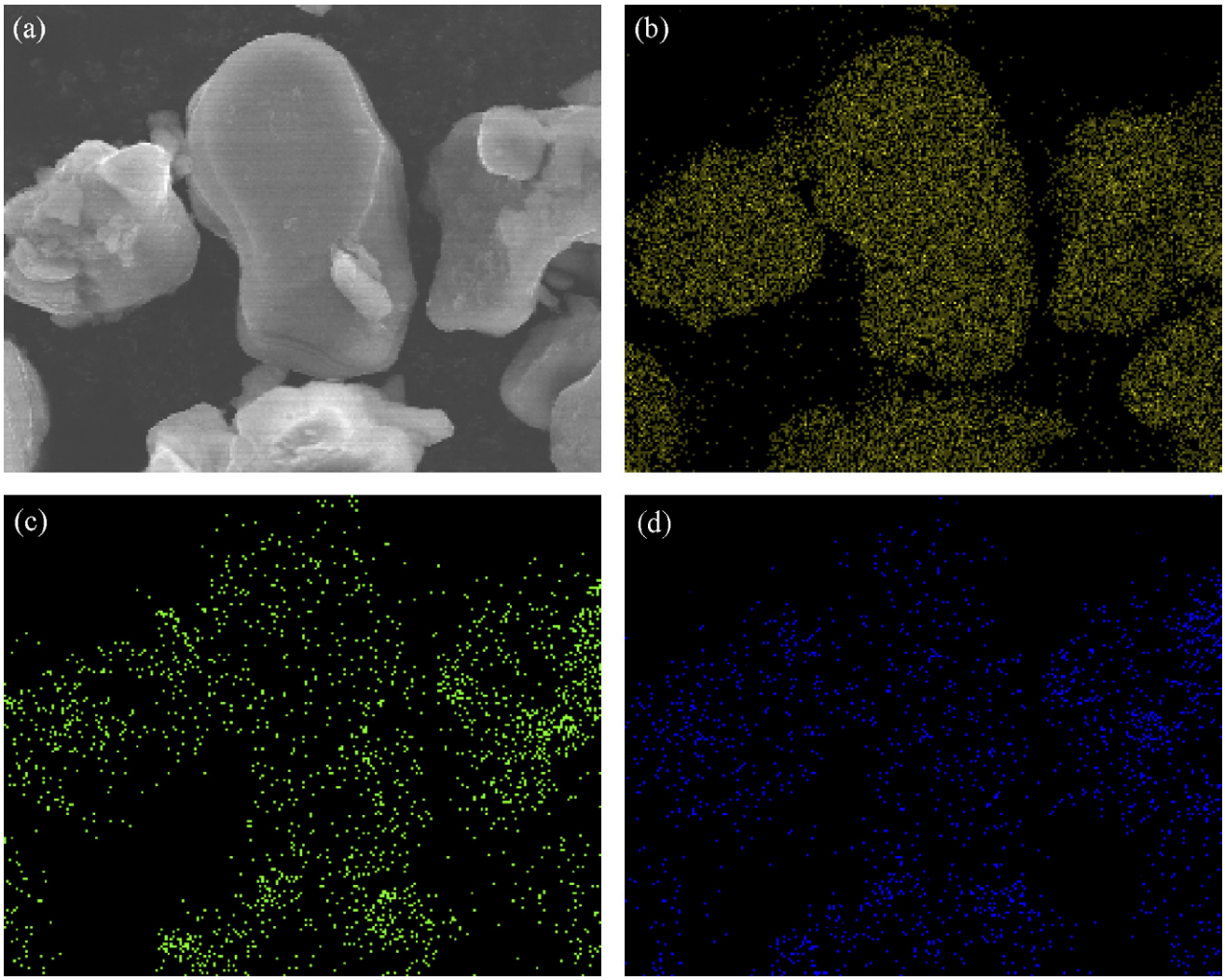

Fig. 5. FE-SEM image (a) and EDS dot-mapping for Co (b), P (c) and Fe (d) elements of the 3 wt.% $FePO_4$-coated $LiCoO_2$ powders.

the $LiCoO_2$ particles is covered by a uniform layer of $FePO_4$ nanoparticles. In contrast with 1 wt.% $FePO_4$-coated $LiCoO_2$ powders, it is seen that the morphologies of 3 and 5 wt.% $FePO_4$-coated ones change apparently even at low magnification (Fig. 4c and d). Fig. 4d also shows that the 5 wt.% $FePO_4$-coated $LiCoO_2$ particles aggregate together slightly. We can note from the inset images of Fig. 4c and d that $FePO_4$ nanoparticles combine together to form an uniform thin film on the surface of 3 and 5 wt.% $FePO_4$-coated $LiCoO_2$ materials, respectively. EDS was performed to check the uniformity of $FePO_4$ coating layer on the surface of 3 wt.% $FePO_4$-coated $LiCoO_2$, it is seen from Fig. 5 that the P and Fe components are almost completely encapsulated on the cathode surface. Fig. 6 presents TEM images of uncoated and 3 wt.% $FePO_4$-coated $LiCoO_2$ particles. The images reveal that the thickness of $FePO_4$ coating layer is about 150 nm, which agrees well with the AES result.

So, we can draw a conclusion that $FePO_4$ coating material exists as an uniform, thin film on the surface of $LiCoO_2$.

3.2. Electrochemical properties

Fig. 7 shows the first cycle discharge profiles of different amounts of $FePO_4$-coated and uncoated $LiCoO_2$ electrodes. When the cells cycle between 2.75 and 4.3 V, the initial discharge specific capacities of 0, 1, 3 and 5 wt.% $FePO_4$-coated materials are 150, 148, 146 and 125 mAh g^{-1}, respectively. We can note that the capacities of 1 and 3 wt.% $FePO_4$-coated materials are slightly lower than that of the uncoated, but the capacity of 5 wt.% $FePO_4$-coated material is largely decreased by ~25 mAh g^{-1}, probably because the relatively thicker $FePO_4$ coating layer hinders the intercalation and deintercalation of lithium during charge–discharge process. When the charge cutoff voltage is increased to 4.4 V, the initial discharge specific capacities of 0, 1, 3 and 5 wt.% $FePO_4$-coated materials are 159, 157, 155 and 144 mAh g^{-1}, respectively. As the charge cutoff voltage is increased by 0.1 V, the discharge capacity increases by ~9 mAh g^{-1}, while 5 wt.% $FePO_4$-coated $LiCoO_2$ ~19 mAh g^{-1}.

The coating effect on the cycle-life of the cathode materials was studied as a function of the $FePO_4$ coating level. Fig. 8A shows the cycling performance of $FePO_4$-coated and uncoated $LiCoO_2$ between 2.75 and 4.3 V at a constant 1 C current. As for pristine $LiCoO_2$, the specific discharge capacity fades to 108.7 mAh g^{-1} at the 400th cycle with a capacity retention ratio of 72.5%. In the case of $FePO_4$-coated materials, the discharge capacities at the 400th cycle decrease to 134.4, 129.3 and 84.5 mAh g^{-1} with capacity retention ratios of 90.6, 88.7 and 67.7%, for coating levels of 1, 3 and 5 wt.%, respectively. It is apparently that 1 and 3 wt.% $FePO_4$ coating show a beneficial effect on improving the cycling performance of $LiCoO_2$. However, the cycling performance of 5 wt.% $FePO_4$-coated $LiCoO_2$ is worse than that of the uncoated $LiCoO_2$. The reason is

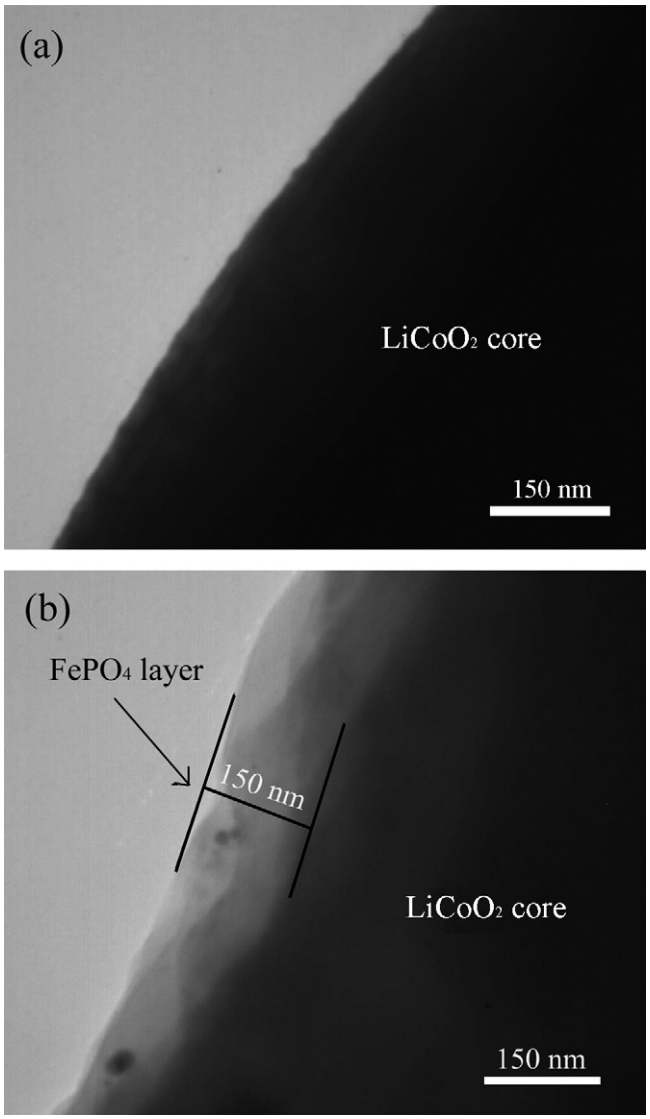

Fig. 6. TEM images of (a) uncoated and (b) 3 wt.% $FePO_4$-coated $LiCoO_2$ particles.

that the thicker the $FePO_4$ coating layer becomes, the more difficult the intercalation and deintercalation of lithium is. As the amount of $FePO_4$ coating layer is increased to 5 wt.%, the coating layer is so thick that it obstructs the transportation of lithium, which makes the irreversible capacity become larger and the cycling performance worse.

In order to examine the cycling behavior of the $FePO_4$-coated $LiCoO_2$ materials in a wider voltage range, the charge cutoff voltage was set at 4.4 V. The cycling performance of $FePO_4$-coated and uncoated $LiCoO_2$ samples between 2.75 and 4.4 V is shown in Fig. 8B. The discharge capacities of uncoated and 5 wt.% $FePO_4$-coated $LiCoO_2$ sharply fade to 106.1 and 57.7 mAh g^{-1} at the 300th cycle, respectively, while the capacities of 1 and 3 wt.% $FePO_4$-coated $LiCoO_2$ only decrease to 116 and 128 mAh g^{-1} at the 400th cycle, corresponding to capacity retention ratios of 73.8 and 82.6%. It is evidently that the cycling performance of 1 and 3 wt.% $FePO_4$-coated $LiCoO_2$ is much better than that of the uncoated, which means that the anti-overcharge performance is greatly enhanced. When the cell is charged to a high potential, a large amount of Co^{3+} will convert to Co^{4+} in $LiCoO_2$ structure. If the cathode material is exposed to the electrolyte, the strong oxidizing Co^{4+} will react with the electrolyte and lead to a rapid capacity loss. The uniform $FePO_4$ coating layer can prevent Co^{4+} from direct contact with the electrolyte and greatly decrease the capacity loss [22].

Fig. 9A and B shows the plots of dQ/dV versus voltage for the pristine and 3 wt.% $FePO_4$-coated $LiCoO_2$ cathode between 2.75 and 4.3 V at the 1st and 350th cycle, respectively. From Fig. 9A, it is observed that the charge–discharge peaks of the pristine $LiCoO_2$ are centered at 3.97 and 3.65 V, respectively, and the peaks are narrow and sharp. However, after 350 cycles, it is shown that the transition peaks become broader and shift to 4.08 and 3.60 V. As for 3 wt.% $FePO_4$-coated $LiCoO_2$ cathode (Fig. 9B), the peaks corresponding to the phase transition during charge–discharge process are centered at 4.03 and 3.61 V, respectively, are narrow and sharp, whereas after 350 cycles, the peaks only shift to 4.05 and 3.57 V, are still narrow and sharp. From Fig. 9A and B, we can also see that the voltage gap (ΔV) of uncoated $LiCoO_2$ is increased from 0.32 to 0.48 V, while that of 3 wt.% $FePO_4$-coated $LiCoO_2$ is increased by only 0.06 V. Fig. 9C and D shows the plots of dQ/dV versus voltage for the pristine and 3 wt.% $FePO_4$-coated $LiCoO_2$ cathodes between 2.75 and 4.4 V at the 1st and 350th cycle, respectively. From Fig. 9C, we can see that the charge–discharge peaks of the pristine $LiCoO_2$ are centered at 3.97 and 3.63 V, respectively. However, after 350 cycles, the peaks become so broad that the charge plateau almost disappears, and the voltage gap (ΔV) between charge and discharge peaks is increased from 0.34 to 0.81 V. It is evident that the structure of $LiCoO_2$ is destroyed severely during the charge–discharge process between 2.75 and 4.4 V. In comparison with uncoated $LiCoO_2$,

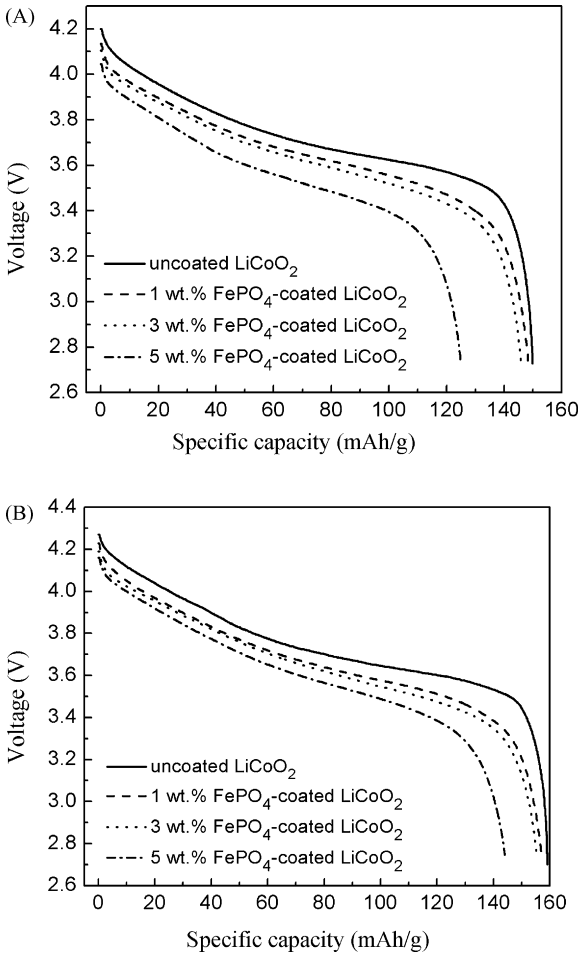

Fig. 7. The initial discharge curves of 0, 1, 3 and 5 wt.% $FePO_4$-coated $LiCoO_2$ in the voltage range of (A) 2.75–4.3 V and (B) 2.75–4.4 V.

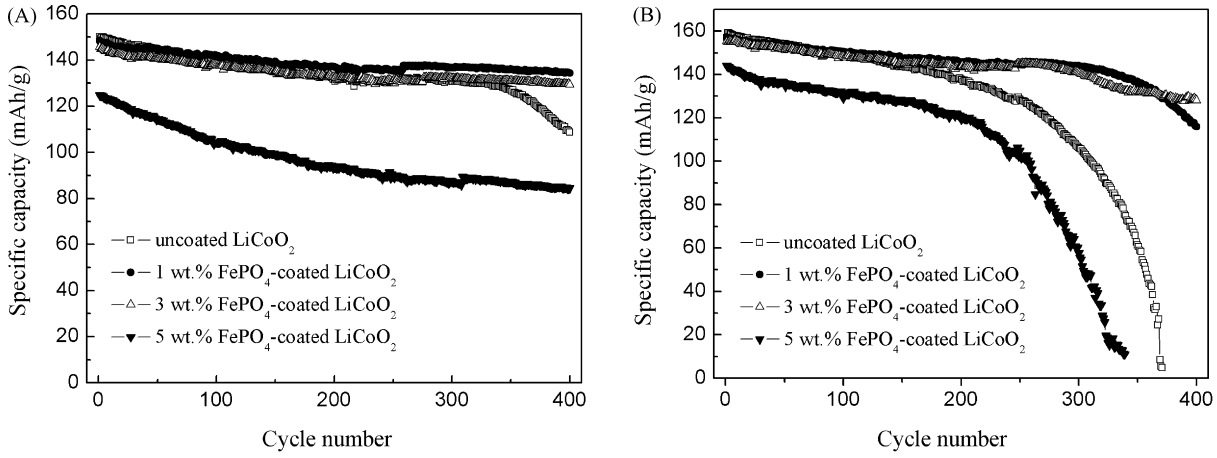

Fig. 8. Cyclic performances of 0, 1, 3 and 5 wt.% $FePO_4$-coated $LiCoO_2$ in the voltage range of (A) 2.75–4.3 V and (B) 2.75–4.4 V.

the charge–discharge peaks of 3 wt.% $FePO_4$-coated $LiCoO_2$ are centered at 4.03 and 3.61 V, respectively, whereas after 350 cycles, the voltage gap (ΔV) only changes from 0.42 to 0.52 V. Because the charge–discharge plateaus strongly depend on the structure of the cathode, based on the above results, we can draw a conclusion that the $FePO_4$ coating layer is very helpful to stabilize the structure of the $LiCoO_2$ cathode during the charge–discharge process in a wider charge–discharge cutoff voltage range.

Moreover, we can conclude that the electrochemical performance of 3 wt.% $FePO_4$-coated $LiCoO_2$ is the best. So other experiments including EIS and safety performance tests were performed using 3 wt.% $FePO_4$-coated $LiCoO_2$ material.

The EIS for the pristine and $FePO_4$-coated $LiCoO_2$ cathodes with cycle number were measured at the charged state of 4.3 V versus Li, as shown in Fig. 10. As Aurback and co-workers' studies on EIS of $LiCoO_2$ [23], each impedance spectrum of the uncoated and 3 wt.%

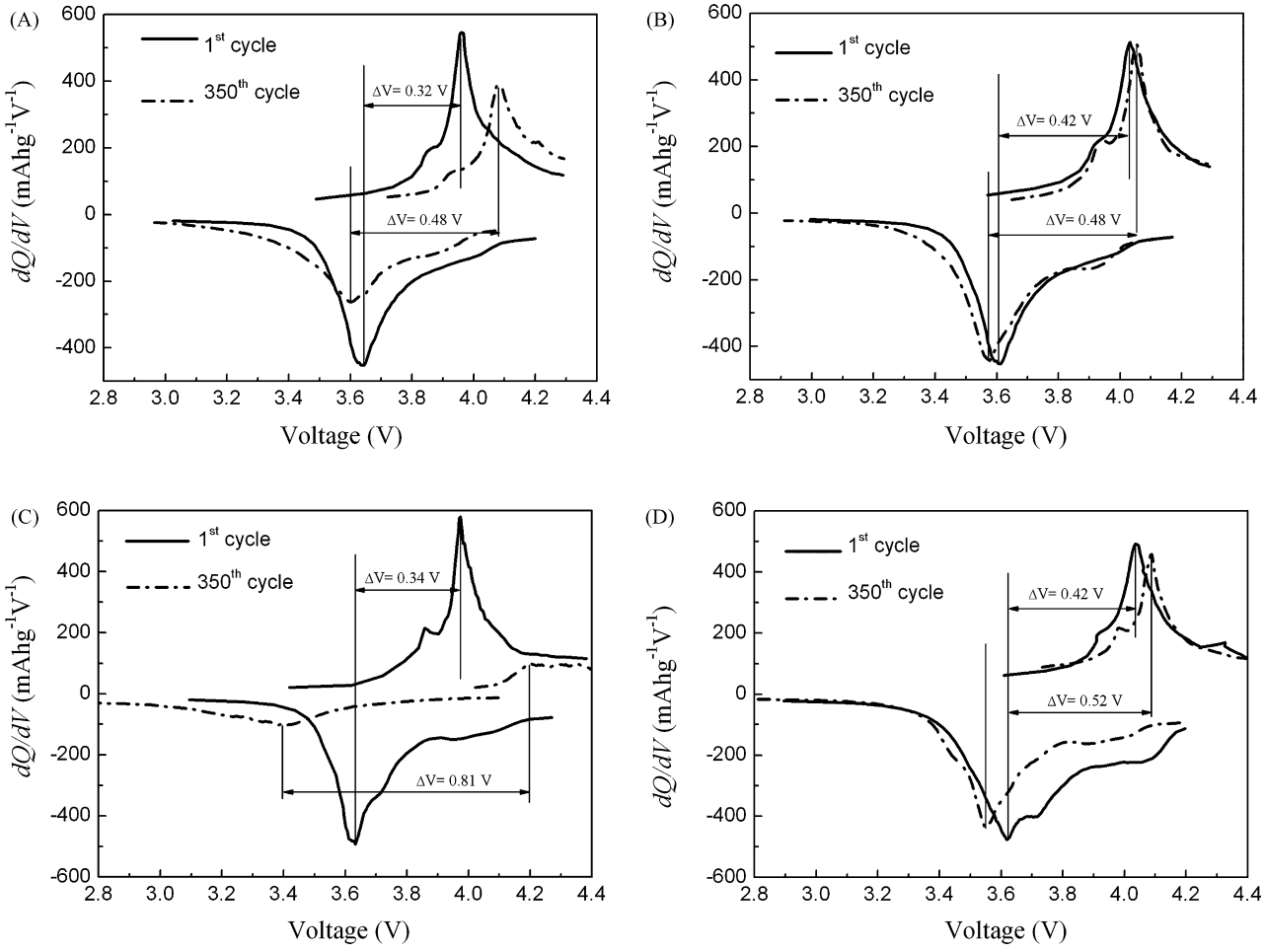

Fig. 9. The dQ/dV vs. voltage curves of uncoated and 3 wt.% $FePO_4$-coated $LiCoO_2$ in the voltage range of: (A) and (B) 2.75–4.3 V, (C) and (D) 2.75–4.4 V.

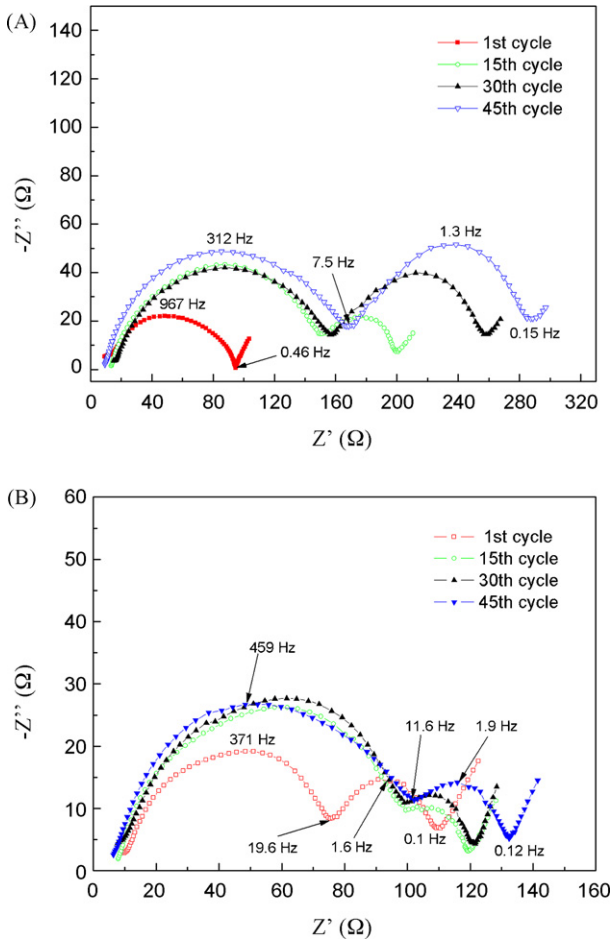

Fig. 10. Nyquist plots of (A) Li/uncoated $LiCoO_2$ and (B) Li/3 wt.% $FePO_4$-coated $LiCoO_2$ cells at the 1st, 15th, 30th and 45th cycle.

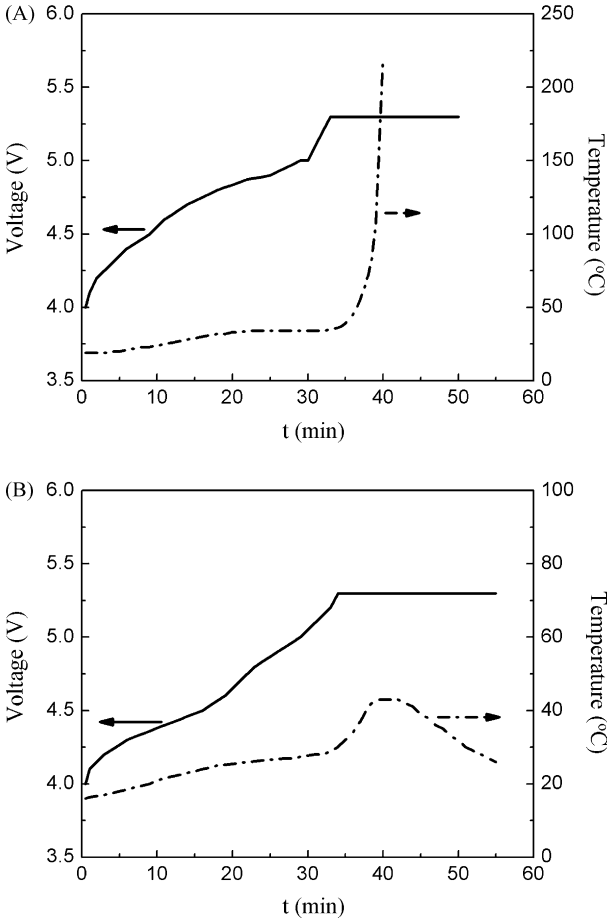

Fig. 11. 3 C overcharge profiles of the cells with (A) uncoated $LiCoO_2$ cathode and (B) 3 wt.% $FePO_4$-coated $LiCoO_2$ cathode.

$FePO_4$-coated $LiCoO_2$ electrodes consists of three parts: a semicircle in the high frequency range which reflects the resistance to Li^+ ion migration through the solid-electrolyte interfacial (SEI) film and film capacitance; another semicircle in the medium-to-low frequency range due to charge-transfer resistance and interfacial capacitance between the electrode and the electrolyte; and a sloping line at low frequency range which reflects Li^+ ion diffusion in the solid electrode. From Fig. 10, we can see that the variation tendency of the high frequency semicircles of the uncoated and 3 wt.% $FePO_4$-coated $LiCoO_2$ is similar, which is that the diameter of the high frequency semicircle at the 1st cycle is small, then increases, and levels off as the charge–discharge cycling proceeds, and the reason is that the SEI film has basically formed during the first several cycles and changes very little during the following cycles. However, the diameter of the high frequency semicircle of 3 wt.% $FePO_4$-coated $LiCoO_2$ cathode is slightly smaller than that of the uncoated cathode, and the reason may be that the interfacial structure of $LiCoO_2$ has been changed after modified with $FePO_4$, which further changes the interfacial properties of $LiCoO_2$.

However, the main difference between the uncoated and 3 wt.% $FePO_4$-coated $LiCoO_2$ electrode lies in the variation tendency of medium-to-low frequency semicircle, which represents the charge-transfer resistance. It is seen clearly from Fig. 10A that the medium-to-low frequency semicircle of the uncoated $LiCoO_2$ electrode does not appear at the 1st cycle, which shows that the charge transfer impedance is very small. However, the diameter of the medium-to-low frequency semicircle of the uncoated $LiCoO_2$ electrode increases endlessly during the following microscope cycles and becomes much larger than that of 3 wt.% $FePO_4$-coated $LiCoO_2$ electrode. From Fig. 10B, we can see that though the diameter of medium-to-low frequency semicircle of 3 wt.% $FePO_4$-coated $LiCoO_2$ electrode at the 1st cycle is larger than that of the uncoated $LiCoO_2$ electrode, it changes very little during the following charge–discharge cycles. So, we can conclude that the charge transfer impedance of 3 wt.% $FePO_4$-coated $LiCoO_2$ electrode

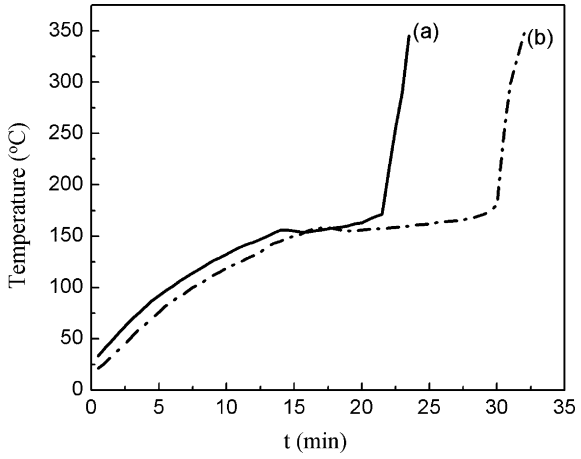

Fig. 12. Hot-box test profiles of the cells with (a) uncoated $LiCoO_2$ cathode and (b) 3 wt.% $FePO_4$-coated $LiCoO_2$ cathode.

keeps stable during the charge–discharge process, while that of the uncoated electrode continually increases, and the reason may be that the $FePO_4$ coating layer can not only effectively suppress the decomposition of the electrolyte solution on the charged particle surface, but also partially absorb the stress resulted from the volumetric change of the granules during the cycling, thereby reduce the strain of the binder/conductive agent and suppress the formation of the voids between the binder/conductive agent and active material particles [24]. Therefore, 3 wt.% $FePO_4$-coated $LiCoO_2$ powders possess better electrochemical cycling performance than that of the uncoated $LiCoO_2$.

3.3. Safety performance

In order to determine the effect of $FePO_4$ coating layer on the safety performance of $LiCoO_2$, 3 C overcharge and hot-box experiments were performed. It is found through many experiments that the charge voltage of both 3 wt.% $FePO_4$-coated and uncoated $LiCoO_2$ cannot surpass 5.3 V, since the critical voltage strongly depends on the nature of $LiCoO_2$. Based on this result, we chose 5.3 V as the highest charge cutoff voltage in the following experiments.

It is seen clearly that the cell containing uncoated $LiCoO_2$ cathode (Fig. 11A) shows thermal runaway with the surface temperature of the cell over 220 °C during the overcharge test, while that of the cell with 3 wt.% $FePO_4$-coated cathode (Fig. 11B) increases to only ~43 °C without burning the cell. Fig. 12 shows the hot-box experiment results of the cells with both pristine $LiCoO_2$ and $FePO_4$-coated $LiCoO_2$ cathodes, respectively. Though both of the cells with uncoated and 3 wt.% $FePO_4$-coated $LiCoO_2$ cathodes exploded in the end, the explosive time of the cell with 3 wt.% $FePO_4$-coated cathode is prolonged from 20 to 30 min. The above results indicate that the $FePO_4$ coating layer is beneficial to enhance anti-overcharge and thermal safety performance.

The reason that the $FePO_4$-coated $LiCoO_2$ is superior to bare $LiCoO_2$ may be attributed to the strong P=O bond (bond energy = 5.64 eV) which is very resistant to chemical attack [13]. High thermal stability of the $FePO_4$ layer may be attributed to the strong covalency of the PO_4^{3-} polyanions with the Fe^{3+} ions in $FePO_4$.

When the cell is charged to high potential, a large portion of Co^{3+} will convert to Co^{4+} in $LiCoO_2$ structure. If the charged cell is placed in a 145 °C oven, the strong oxidizing Co^{4+} cations will react with the electrolyte, and the cell will generate amounts of heat. The thick $FePO_4$ coating layer on the $LiCoO_2$ cathodes blocked the thermal runaway of the Li-ion cell and significantly reduced the electrolyte oxidation as well as Co dissolution into the electrolyte [25].

4. Conclusions

A commercial $LiCoO_2$ is successfully coated with different amounts of $FePO_4$ by a coprecipitation method. When the charge cutoff voltage is increased to 4.3 and 4.4 V, 3 wt.% $FePO_4$-coated $LiCoO_2$ still has a good electrochemical performance with initial discharge capacities of 146 and 155 mAh g^{-1} and superior capacity retention ratios of 88.7 and 82.5% after 400 cycles, respectively. The dQ/dV versus voltage curves indicate that the $FePO_4$ coating layer is very helpful to stabilize the structure of $LiCoO_2$ during the charge–discharge process. EIS spectrum indicates that the $FePO_4$ coating layer greatly restrains the charge transfer impedance growth of the cell, resulting in an enhanced cycling stability. The 3 C overcharge and hot-box results expose that the $FePO_4$ coating layer could also enhance the anti-overcharge and thermal stability of $LiCoO_2$.

Acknowledgements

This work was supported by the National Natural Science Foundation of China, the National 863 Project (Grant No. 2006AA03Z343), the 111 Project (Grant No. B07004), and the Program for Changjiang Scholars and Innovative Research Teams in Universities (Grant No. IRT0406).

References

[1] T. Ohzuku, R.J. Brodd, J. Power Sources 174 (2007) 449.
[2] Q. Cao, H.P. Zhang, G.J. Wang, Q. Xia, Y.P. Wu, H.Q. Wu, Eletrochem. Commun. 9 (2007) 1228.
[3] H. Wang, M.C. Chen, Electrochem, Solid State Lett. 9 (2006) A82.
[4] H. Lee, M.G. Kim, J. Cho, Eletrochem. Commun. 9 (2007) 149.
[5] Y.-I. Jang, N.J. Dudney, D.A. Blom, L.F. Allard, J. Electrochem. Soc. 149 (2002) A1442.
[6] Y.I. Jang, B. Huang, D.R. Sadoway, G. Ceder, Y.-M. Chiang, H. Lui, H. Tamura, J. Electrochem. Soc. 146 (1999) 862.
[7] H. Tukamoto, A.R. West, J. Electrochem. Soc. 144 (1997) 3164.
[8] M. Zou, M. Yoshio, S. Gopukumar, J.-I. Yamaki, Chem. Mater. 15 (2003) 4699.
[9] M. Mladenov, R. Stoyanova, E. Zhecheva, S. Vassilev, Eletrochem. Commun. 3 (2001) 410.
[10] S. Oh, J.K. Lee, D. Byun, W.I. Cho, B.W. Cho, J. Power Sources 132 (2004) 249.
[11] H.W. Ha, K.H. Jeong, N.J. Yun, M.Z. Hong, K. Kim, Electrochim. Acta 50 (2005) 3764.
[12] S.M. Lee, S.h. Oh, J.P. Ahn, W.I. Cho, H. Jang, J. Power Sources 159 (2006) 1334.
[13] J. Cho, Y.W. Kim, B. Kim, J.G. Lee, B. Park, Angew. Chem. Int. Ed. 42 (2003) 1618.
[14] J. Cho, Y.J. Kim, B. Park, Chem. Mater. 12 (2000) 3788.
[15] T. Fang, J.G. Duh, Surf. Coat. Technol. 201 (2006) 1886.
[16] J. Cho, Y.J. Kim, B. Park, J. Electrochem. Soc. 148 (2001) A1110.
[17] H. Wang, W.D. Zhang, L.Y. Zhu, M.C. Chen, Solid State Ionics 178 (2007) 131.
[18] Y.S. Hong, K.S. Ryu, Y.J. Park, M.J. Kim, J.M. Lee, S.H. Chang, J. Mater. Chem. 12 (2002) 1870.
[19] Y. Song, P.Y. Zavalij, M. Suzuki, M.S. Whittingham, Inorg. Chem. 41 (2002) 5778.
[20] Z.C. Shi, A. Attia, W.L. Ye, Q. Wang, Y.X. Li, Y. Yong, Electrochim. Acta 53 (2008) 2665.
[21] M. Holzapfel, R. Schreiner, A. Ott, Electrochim. Acta 46 (2001) 1063.
[22] L.J. Liu, Z.X. Wang, H. Li, L.Q. Chen, X.J. Huang, Solid State Ionics 152–153 (2002) 341.
[23] M.S. Levi, G. Salitra, B. Markovsky, H. Teller, D. Aurback, U. Heider, L. Heider, J. Electrochem. Soc. 146 (1999) 1279.
[24] D.C. Li, Y. Kato, K. Kobayakawa, H. Noguchi, Y. Sato, J. Power Sources 160 (2006) 1342.
[25] J. Cho, H. Kim, B. Park, J. Electrochem. Soc. 151 (2004) A1707.